Design study of an improved laser wire system for electron beam measurement*

WU Dai(吴岱)[1,2;1)] YANG Ren-Jun(杨仁俊)[1] BAI Wei(柏伟)[1] LI Peng(李鹏)[1]
LI Ming(黎明)[1] YANG Xing-Fan(杨兴繁)[1]

[1] Institute of Applied Electronics, China Academy of Engineering Physics, Mianyang 621900, China
[2] Department of Engineering Physics, Tsinghua University, Beijing 100084, China

Abstract: The laser wire (LW) method has been demonstrated to be an effective non-interceptive technique for measuring transverse profile and emittance of electron beams in colliders, storage rings and dumping rings. In this paper, we present an improved design of high repetition LW system for high average power free electron lasers (HAP FELs) and energy recovery linacs (ERLs). This improved LW utilizes the excess power of the photocathode drive laser, thus making itself much cheaper and simpler. The system main parameters are optimized with numerical calculations and Monte Carlo simulations, indicating that resolutions would be better than 100 μm and scanning time less than 1 minute. Status of the experiment preparation is also presented.

Key words: laser wire, electron beam transverse profile, Compton scattering, FEL-THz

PACS: 29.27.Fh, 41.60.Cr, 13.60.Fz **DOI:** 10.1088/1674-1137/37/10/108101

1 Introduction

In the future high average power free electron lasers (HAP FELs) and energy recovery linacs (ERLs), electron beams have a high repetition rate from MHz to GHz and an MW-grade power, which will destroy any target arranged for measurements [1–3]. As a result, the determination of basic electron beam properties including transverse profile, emittance and bunch length should be noninvasive. The normal technologies, such as OTR screens [4], scintillation monitors [5], deflecting cavities [6] and wire scanners [7] are inapplicable. One advanced method for noninvasive beam size and emittance diagnostic is the laser wire (LW) scanner [8–11], which is based on laser-electron Compton scattering.

A number of LW systems have been developed in multi-GeV colliders, dumping rings, spallation neutron sources, and also have found applications in the Thomson regime at lower energy [11–18]. There are two major LW methods: one is to intercept electron beams with continuous wave (CW) laser in an optical cavity for storage rings [13, 14] and the other with a high power single laser pulse for linacs [9, 12, 17, 18]. However, neither of them is optimal for the diagnostics of electron beams with MHz repetition rate in HAP FELs or ERLs. The single pulse LW requires special care of the optical components to endure high energy density laser pulse and thus it is obviously expensive. The scan speed is limited by the laser repetition rate and the impact on the beam is rather strong. The CW LW needs complicated optical cavity technologies and most of the laser power will be lost in the intervals between electron bunches. Plus, neither of them can measure the bunch length because of the jitter among RF field, electron beams and laser field. Furthermore, they cannot distinguish beams with different energies which are very close in ERLs.

In order to avoid the disadvantages mentioned above, Murokh [19] and Evtushenko [20] proposed a high repetition LW for BNL ERL and JLab's HAP FEL, respectively. This new-type LW improves the scattered photon yield by improving the repetition frequency, and becomes faster and more-efficient. The only drawback is that it needs a new mode-locked laser system fitting to the electron beams, which makes it relatively expensive and its jitter unpredictable.

In this paper, an improved high repetition LW system, which utilizes the excess power of the photocathode drive laser, is presented and analyzed, and its design study in China Academy of Engineering Physics (CAEP) is introduced. This improved one can be much cheaper, faster, naturally mode-locked and may be suitable for beam longitudinal diagnostics because the average effect cancels the jitter.

The paper is organized as follows: The system layout

Received 12 December 2012
* Supported by Development Foundation of CAEP (2011B0402070)
1) E-mail: wudai04@163.com

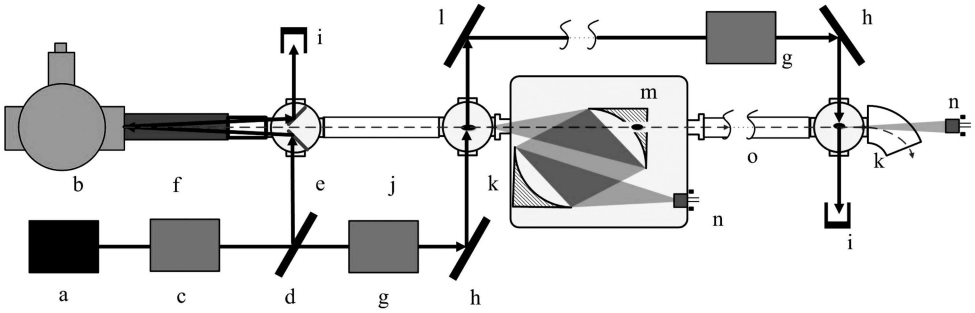

Fig. 1. Layout of the improved CAEP high repetition LW facility (not to scale). a: The laser system; b: The photocathode high-voltage DC electron gun; c: The laser transmission path; d: The laser splitter; e: The drive laser incident cavity; f: The solenoid magnet; g: The laser delay system; h: The laser scanning system; i: The laser dump; j: The electron drift tube; k: The laser-electron interaction cavity; l: The deflecting mirror; m: The scattered photon detective cavity; n: PMT and o: The accelerator tubes.

and the main innovation are introduced in Section 2; then the design parameters, calculations and simulations are studied in Section 3; finally, the progress of experiment preparation is given in Section 4.

2 System layout and the main innovation

Layout of the CAEP high repetition LW facility is shown in Fig. 1.

This system is going to be installed on the CAEP FEL-THz facility [21]. A 54.167 MHz drive laser system generates short pulse with 532 nm wavelength for electron production. A JLab type photocathode high-voltage DC gun is used to generate 200–350 keV, high quality electron bunches [22]. The photocathode material is GaAs, of which the quantum efficiency (QE) would be 0.5%–10%. To generate 1 mA CW electron beam, 23 mW–0.47 W laser power is needed.

The average output power of the drive laser is 8 watts. The excess laser power can be used to build a laser wire scanner to measure the electron beams. The laser is separated into two parts: one reaches the cathode surface, the other passes through the laser delay and scan systems, and collides with the electron beam in the interaction cavities. The photoelectric multiplier tubes (PMTs) are used to count the scattered photons. The photons before the accelerator are collected by a detective cavity, while the ones after the accelerator are separated from electron beam by a dipole magnet. The counting rate of scattered photons is:

$$R_{\rm sc}=f\cdot(N_{\rm sc}), \tag{1}$$

where $N_{\rm sc}$ is the photon yield in each Thomson scattering and f is the colliding frequency, which is exactly equal to the laser and electron repetition.

This naturally mode-locked system reduces complexity and takes advantage of the extra laser power, thus making itself much cheaper and simpler. The megahertz repetition can improve the scanning speed and reduce the jitter because of the average effect. In the ERLs, electron beams with different energies are arranged in very small intervals, so only this mode-locked laser probe can measure them separately. Furthermore, $N_{\rm sc}$ is very small, which means that the impact on the electron beam can be ignored.

3 Calculation and simulation

3.1 Design parameter

The optimized electron pulses qualities, laser qualities and main machine parameters are listed in Table 1. We use the code PARMELA [23] to simulate the dynamics of electrons subject to static electric field, RF field, magnetic field, and their self-field. Some of the optimization simulations can be found in Ref. [24], while others are under publication.

Table 1. The CAEP LW facility parameters.

parameters	value
physical dimension	
from gun cathode to interaction point one	90.6 cm
from gun cathode to interaction point two	450 cm
electron pulse at interaction point one	
bunch radius/(Guassian, rms)	1 mm
bunch length/(Guassian, rms)	8 ps
bunch charge	90 pC
bunch kinetic energy	200–350 keV
electron pulse at interaction point two	
bunch radius/(Guassian, rms)	1 mm
bunch length/(Guassian, rms)	3 ps
bunch charge	90 pC
bunch kinetic energy	6–8 MeV
laser at interaction point one and two	
average power	3 W
transverse radius/(Guassian, rms)	25 μm
longitudinal size/(Guassian, rms)	6.4 ps
repetition	54.167 MHz

3.2 Numerical analysis

We consider the colliding of a single laser beam with an electron beam bunch having electron number $N_{\rm e}$, as shown in Fig. 2. The electron's relativistic factor is γ and the laser photon energy is $h\nu_0$. The root mean square (rms) dimensions of the electron beam are σ_x, σ_y and σ_z (considered as a Guassian distribution). The laser beam is assumed to be an ideal circular distribution, with an rms length $\sigma_{\rm L}$ and a waist size $\sigma_{\rm w}$. When the laser scans the electron beam along y axis, the distance between both centers is δy.

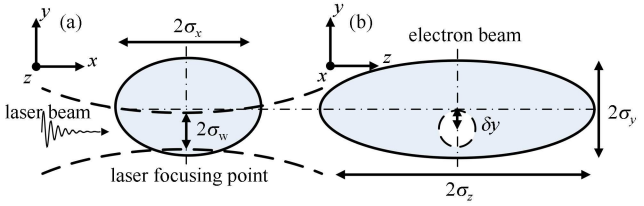

Fig. 2. The laser-electron colliding detail in x-y plane (a) and in y-z plane (b).

The scattered photon number is written as [25]:

$$N_{\rm sc}(\delta y)=s(\delta y)N_{\rm sc}(0), \tag{2}$$

with

$$s(\delta y)=\exp\left[-\frac{\delta y^2}{2\left(\sigma_y^2+\sigma_{\rm w}^2\right)}\right], \tag{3}$$

$$N_{\rm sc}(0)=\frac{\sqrt{2}\sigma_c P_0 N_{\rm e}\sigma_{\rm L}\Delta\lambda/\lambda}{ch\nu_0\sqrt{\pi(\sigma_y^2+\sigma_{\rm w}^2)(\sigma_z^2+\sigma_x^2+\sigma_{\rm L}^2+\sigma_{\rm w}^2)}}, \tag{4}$$

where P_0 is the laser peak power, σ_c is the Compton cross section, c is the light speed in vacuum and $\Delta\lambda/\lambda$ is the spectral width in the acceptance angle. By counting the scattered photon numbers with different δy, the distribution of the electron density along y-axis can be reconstructed when $\sigma_y \gg \sigma_{\rm w}$.

The scattered photon's energy is given by

$$h\nu_{\rm sc}=\frac{h\nu_0\gamma(1-\beta\cos\psi)}{\gamma(1-\beta\cos\theta)+h\nu_0[1-\cos(\psi-\theta)]/E_0}, \tag{5}$$

where E_0 is the electron rest energy, β is the electron's relativistic velocity, ψ is the collision angle between the electron and the laser beam, and θ is the observation angle in the laboratory frame.

Figure 3 shows the numerical results of LW scanning with different $\sigma_{\rm w}$ according to Eqs. (2)–(4). The line $\sigma_{\rm w}/\sigma_y=0$ represents the real electron density distribution. The calculation confirms that when $\sigma_{\rm w} \ll \sigma_y$, the scanning result is the electron beam density distribution, approximately.

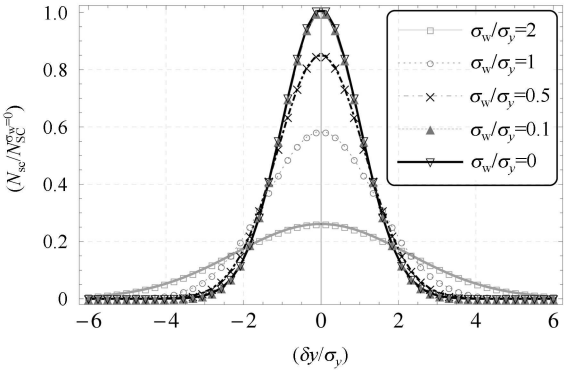

Fig. 3. (color online) The numerical Laser Wire scanning result with different $\sigma_{\rm w}$.

The wavelength of scattered photon ($\lambda_{\rm sc}$) versus the observation angle (θ) and electron energy (E_k) is shown in Fig. 4. Assuming that the wavelength of the laser beam is 532 nm, some of the scattered photons are in the vacuum ultra-violet (VUV) region, which means they can be detected by PMTs.

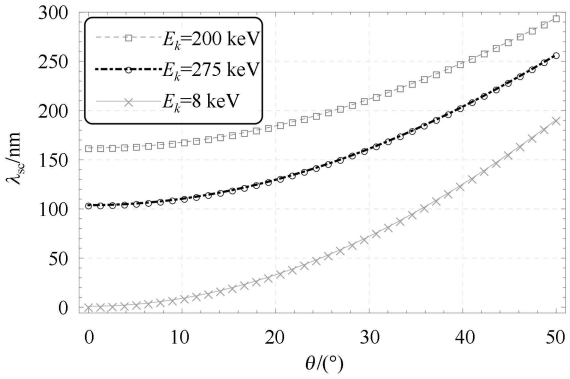

Fig. 4. (color online) The Compton scattered photon wavelength versus the observation angle.

The numerical results are shown in Table 2. In the calculation, $\Delta\lambda/\lambda$ is assumed to be 0.1. The counting rate of the scattered photon is enough for single photon counting (SPC) system, which works in the kilo-Hertz range, indicating that a single measurement can be finished in 1 minute.

Table 2. The numerical results for CAEP high repetition LW system.

position/cm	E_k/MeV	$(\lambda_{\rm sc})_{\rm min}$/nm	$R_{\rm sc}(\delta y=0)/{\rm s}^{-1}$
90.6	0.2	162.1	5495
90.6	0.35	103.8	5993
450	6	1.64	6675
450	8	0.96	6679

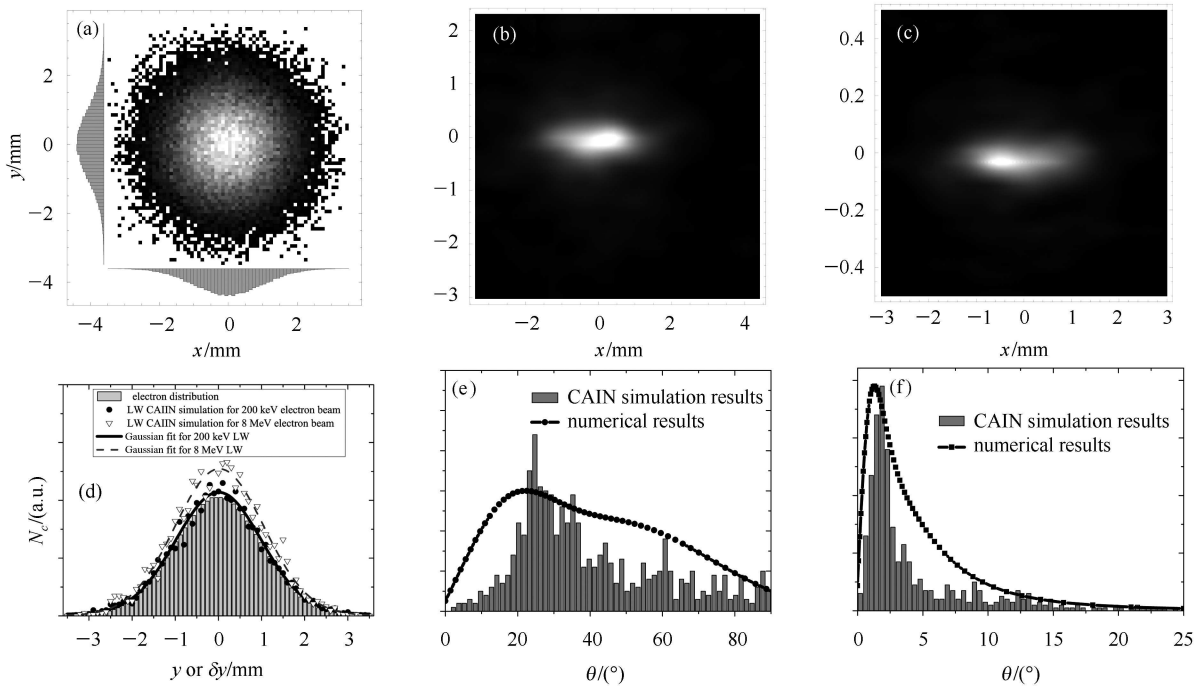

Fig. 5. The CAIN simulation results. (a) is the electron beam density distribution ($\sigma_x = \sigma_y = 1$ mm); (b) and (c) are the scattered photon density distribution; (d) is the normalized scattered photon number versus δy compared with electron density distribution in y direction; (e) and (f) are the normalized scattered photon number versus θ.

3.3 CAIN simulation

We use the Monte Carlo code CAIN [26] to simulate the LW process. In this simulation, parameters in Table 1 are used as the input conditions and the macro-electron number is 6×10^6. As $R_{\rm sc} \propto f \cdot P_0$, the pulse energy of laser is raised up to 3 J in order to simulate high repetition scattering in one single shot. The results are shown in Fig. 5, where pictures in the same row have the same y-axis. N_c means the number of macro-particle counting. Some numerical curves are also posted.

From Fig. 5, one can see that the acceptance angle of scattered photon is reduced obviously when E_k is increased from 200 keV (b) to 8 MeV (c). The same phenomenon is observed in (e) and (f), where the numerical calculations are based on the famous Klein-Nishina formula [27]. The Monte Carlo computation error is greater when the macro-particle number is less, so the counting of scattered photon decreases faster than the numerical calculation.

The basic proof of LW working is shown in Fig. 5 (d), where the photon yields of different energy electron beams have different maximum in order to be distinguished clearly. The Guassian fitting shows that the detected rms radius in y direction would be 1.03 mm when $E_k = 200$ keV and 0.994 mm when $E_k = 8$ MeV, respectively. The results agree well with the actual value.

The simulation shows that the resolution is based on the size of the focal point $\sigma_{\rm w,min}$. With our laser parameters, $\sigma_{\rm w,min}$ can be 25 μm, indicating that the resolution will be less than 100 μm.

4 Status of experiment preparation

The high repetition picosecond laser system is now under commissioning. The power system, the photocathode DC-gun and the GaAs cathode are ready for experiment. The vacuum leak detection of scattered photon detective cavity has been finished. The beamline installation and alignments are to start soon. The laser transport line and scanning system have been constructed. We foresee an improved laser wire prototype experiment early next year. The super-conducting accelerator is going to be installed next year. Then the second LW experiment will be arranged.

5 Summary

In this paper, we have introduced an improved laser wire system which is much cheaper and simpler by utilizing the drive laser to measure the electron beam size, and have presented a design of such a facility at CAEP,

including the system layout, theoretical analysis, numerical calculation and Monte Carlo simulation. The calculation and simulation indicate that the measurement resolutions will be less than 100 μm and the scanning time less than 1 minute. The experiment preparation is in progress. This improved LW system will be a compact and powerful tool for high repetition high average power FELs and ERLs.

References

1 Benson S et al. Nucl. Instrum. Methods Phys. Res. A, 2007, **528**: 14–17
2 Kim K J et al. Phys. Rev. Lett., 2008, **100**: 244802
3 Baptiste K et al. Nucl. Instrum. Methods Phys. Res. A, 2009, **599**: 9–14
4 Wartski, L et al. J. Appl. Phys., 1975, **46**: 3644–3653
5 Young F C et al. Rev. Sci. Instrum., 1977, **48**: 432–443.
6 SHI J, CHEN H, TANG C et al. Chin. Phys. C, 2008, **32**: 205–208
7 Fulton R et al. Nucl. Instrum. Methods Phys. Res. A, 1989, **274**: 37–44
8 Fiocco G, Thompson E, Phys. Rev. Lett., 1963, **10**: 89–91
9 Leemans W P et al. Phys. Rev. Lett., 1996, **77**: 4182
10 Alley R, Arnett D et al. Nucl. Instrum. Methods Phys. Res. A, 1996, **379**: 363-365
11 Telnov V I, Nucl. Instrum. Methods Phys. Res. A, 2003, **513**: 647–650
12 Boscoa A, Price M T et al. Nucl. Instrum. Methods Phys. Res. A, 2008, **592**: 162–170
13 Sakai H, Honda Y et al. Phys. Rev. ST, 2001, **4**: 022801
14 Yosuke H, Noboru S, Sakae A et al. Nucl. Instrum. Methods Phys. Res. A, 2004, **538**: 100–115
15 Lefèvre T, CLIC Note, 2002, **504**: 2001-015
16 Boogert S T et al. Phys. Rev. ST, 2010, **13**: 122801
17 Aryshev A et al. Nucl. Instrum. Methods Phys. Res. A, 2010, **623**: 564–566
18 LIU Y et al. Nucl. Instrum. Methods Phys. Res. A, 2010, **612**: 241–253
19 Murokh A et al. Proc. IPAC, 2010, 1209–1211
20 Evtushenko P. Electron Beam Diagnostics For High Current FEL Drivers. Oral Report of FEL Conference, 2011
21 YANG X et al. Information and Electronic Engineering, 2011, **9**: 361–365
22 WANG H et al. Proc. FEL, 2011, 598–600
23 YOUNG L. PARMELA Manual, LA-UR-96-1835, 1996
24 LI P et al. High Power Laser and Particle Beams, 2012, **23**: 3380–3382 (in Chinese)
25 Kim K J et al. Nucl. Instrum. Methods Phys. Res. A, 1994, **341**: 351–354
26 Yokoya K. User's Manual of CAIN, KEK Pub. 2003
27 Klein O, Nishina Y. Z. Phys., 1929, **52**: 853